identity. The transfer of the H_7 hydrogen atom from the water molecule to the H_3 hydrogen atom to form the hydrogen product molecule occurs in a concerted way with the transfer of the H_5 hydrogen atom from the hydroxyl group to the O_6 oxygen atom regenerating thus a new water molecule. The activation energy of this process obtained at the different levels of calculation are given in the fourth column of Table IV. The comparison of the third and fourth column of that table shows clearly the catalytic effect of the water molecule amounting to about 50 kcal mol^{-1} at the STO-3G and 3-21G levels and to 28 kcal mol^{-1} at the 6-31G** level. Compared with the effect of the polarization functions which do not lower the activation energy, the contribution of electron correlation effects is fairly large and must, therefore, be taken into account for a correct description of the reaction pathway. In fact, at the MP2 6-31G** level, both the calculated activation and reaction energies coincide with the experimental values, respectively 48.5 and −1.36 kcal mol^{-1}. Moreover, one can observe that only the activation energy related to the water-catalyzed decarboxylation mechanism corresponds to the experimental one. That decarboxylation should be catalyzed by a water molecule does not seem inconsistent with the experimental facts since the main channel of the formic acid pyrolysis yields water. Furthermore, given the two mechanisms, the ratio observed in the product yield, i.e., CO/CO_2, could simply be due to the dependence of the decarboxylation on the dehydration reaction and also on the number of effective collisions between the remaining formic acid and the produced water molecules in the gaseous state. From the experimental point of view, this result would suggest that the product ratio could be modified by introducing simultaneously the formic acid and some water vapor into the reactor.

Finally, the large difference between Hsu's decarboxylation activation energy and the one found here and by Blake probably lies in Hsu's kinetic treatment. He determined a second-order rate constant for the decarboxylation in opposition with the first-order rate found by Blake.

Acknowledgment. This work is part of a project funded by the Swiss National Foundation for Scientific Research (Grant No. 3.654-0.84). We gratefully acknowledge the generous assistance of the Centre de Calcul de l'Ecole Polytechnique Fédérale de Lausanne. We express our thanks to Professor J. Weber from the University of Geneva and to Dr. G. Dive from the University of Liège who carried out the MP calculations.

Registry No. Formic acid, 64-18-6.

Photochemistry and Radiation Chemistry of Colloidal Semiconductors. 12. Intermediates of the Oxidation of Extremely Small Particles of CdS, ZnS, and Cd_3P_2 and Size Quantization Effects (A Pulse Radiolysis Study)

S. Baral, A. Fojtik,† H. Weller, and A. Henglein*

Contribution from the Hahn-Meitner-Institut für Kernforschung Berlin, Bereich Strahlenchemie, D-1000 Berlin 39, Federal Republic of Germany. *Received August 7, 1985*

Abstract: The reactions of hydroxyl radicals with colloidal Q-CdS, Q-ZnS, and Q-Cd_3P_2 (materials of extremely small particle size showing optical size quantization effects) were studied pulse radiolytically. The radicals attack the particles at diffusion-controlled rates. In all three cases, a product with a broad absorption band in the visible (sulfides) or near-infrared (phosphide) is formed. This band shifts to shorter wavelengths with decreasing particle size (size quantization effect). It is attributed to surface trapped holes. These holes react with dissolved oxygen. The colloidal particles become a little smaller by OH attack. With use of a CdS sample with a structured absorption spectrum, it is shown that the product particles have their absorption maxima at slightly shorter wavelengths than the reactant particles (size quantization effect).

Radiation chemical studies on colloidal solutions of semiconductor materials allow one to investigate interfacial reactions of free radicals. The radicals are formed in bulk solution and transfer an electron to the colloidal particles. This electron transfer may lead to a cathodic dissolution of the colloid, such as in the case of silver halides.[1] The transferred electrons may be stored for some time and produce a colored material, such as blue TiO_2,[2] or reduce another solute in a two-electron-transfer process.[3] Studies of this kind complement the studies on the photochemistry of such solutions. In the latter case, electrons and positive holes are generated by light absorption and the chemical reactions, which are initiated by these charge carriers, are investigated. The advantage of using radicals for the transfer of electrons is that excess electrons on small particles can be studied without positive holes being present simultaneously.[4,5]

In the present studies, OH radicals are used to inject positive holes into semiconductor particles possessing anions such as S^{2-} and P^{3-} which are readily oxidized. The anodic corrosion is a disturbing problem in the electrochemistry and photoelectrochemistry of compact semiconductor electrodes.[6] To generate OH radicals, colloidal solutions containing nitrous oxide were irradiated. Using the method of pulse radiolysis, one obtains information on the rate of OH attack and on the optical properties and lifetimes of the first intermediates of corrosion. The optical detection of intermediates at compact electrodes is not possible in most cases as the number of species produced in electrochemical experiments is too low. The experiments with colloidal particles

† Home address: Czechoslovak Academy of Sciences, J. Heyrovský Institute of Physical Chemistry and Electrochemistry, Prague, CSSR.

(1) Johnston, F. J. *Rad. Res.* **1978**, *75*, 286-295.
(2) Henglein, A. *Ber. Bunsenges. Phys. Chem.* **1982**, *86*, 241-246.
(3) Gutiérrez, M.; Henglein, A. *Ber. Bunsenges. Phys. Chem.* **1983**, *87*, 474-478.
(4) Henglein, A. In "Photochemical conversion and storage of solar energy"; Rabani, J., Ed.; The Weizmann Science Press of Israel, 1982; Part a, pp. 115-138.
(5) Henglein, A. In "Modern trends of colloid science in chemistry and biology"; Eicke, F., Ed.; Birkhäuser Verlag: Basel, 1985; pp 126-147.
(6) Gerischer, H. "Advances in Electrochemistry and Electrochemical Engineering"; Delahay, P., Ed.; Interscience Publishers: New York, 1961; pp 1, 139-232.

0002-7863/86/1508-0375$01.50/0

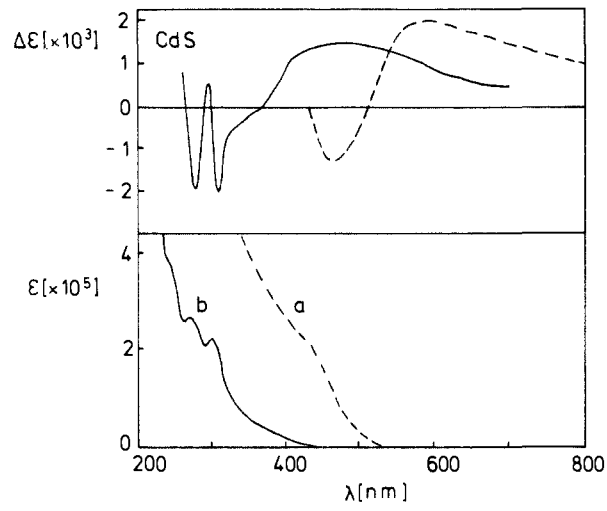

Figure 1. Absorption spectra of CdS sols of different particle sizes (lower part) and change in specific absorbance $\Delta\epsilon$ at 300 μs after the pulse (upper part). Sol a (dashed line): 2×10^{-3} M CdS, 5×10^{-4} M $Na_6(PO_3)_6$, pH 10.5. Sol b (solid line): 1×10^{-4} M CdS, 1×10^{-4} M $Cd(ClO_4)_2$, 2×10^{-4} M $Na_6(PO_3)_6$, pH 8.5. Mean agglomeration numbers: a 266; b, 94.

therefore complement the corrosion studies in electrochemistry.

Special attention is paid in the present paper to the oxidation of "Q-materials". We use this term to designate materials of very small particle size which show size quantization effects due to the restrictions in space of the charge carriers. It has been shown that the optical properties of Q-materials strongly depend on particle size.[7-11] Both the beginning of the light absorption and the fluorescence band are shifted toward shorter wavelengths with decreasing particle size. These materials represent a transition from bulk semiconductor properties to molecular properties. In some cases it was observed that the absorption spectrum contained several maxima spaced by 10 to 20 nm. This was explained by a structured size distribution of the colloids, i.e., the existence of preferential or "magic" agglomeration numbers.[8,11] In the present work, it is shown that the size quantization effects can also be seen in the products of the reaction of hydroxyl radicals with very small colloidal particles.

Experimental Section

The pulse radiolysis apparatus with simultaneous detection of intermediates by optical absorption and conductivity measurements has already been described.[12] In most of the experiments, radicals were generated in a low concentration of 5×10^{-7} M in order to avoid multiple attack of the colloidal particles by the radicals. As the optical signals were very small under these conditions, the signals from a large number of pulses were averaged. The solution slowly streamed through the irradiation vessel to avoid irradiation with more than one pulse. The base line was recorded every other pulse and finally subtracted from the recorded signals.[12]

The colloids were prepared, as recently described, by injecting hydrogen sulfide or phosphine into a deaerated solution of $Cd(ClO_4)_2$ or $Zn(ClO_4)_2$.[8,13] The solution also contained various amounts of sodium hexametaphosphate (Riedel de Haen). The solutions were always freshly prepared. They were bubbled for 30 min with purified nitrous oxide or with an 80 to 20% mixture of nitrous oxide and oxygen. N_2O reacts with hydrated electrons from the radiolysis of the aqueous solvent according to

$$N_2O + e^-_{aq} \rightarrow N_2 + OH + OH^- \quad (1)$$

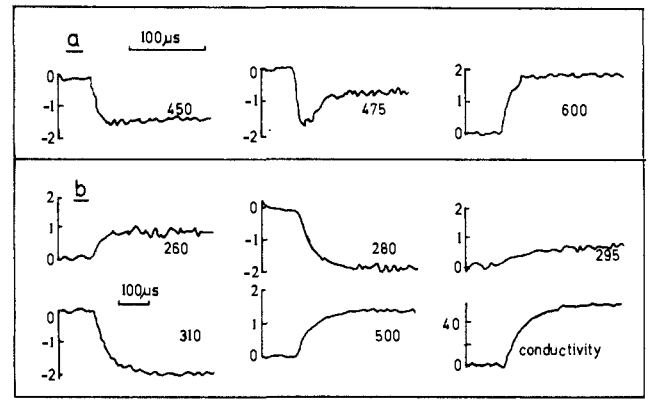

Figure 2. Digitizer traces of samples a and b (Figure 1) at various wavelengths. The vertical axis is given in $\Delta\epsilon$ [$\times 10^3$]. The trace for conductivity is given in Ω^{-1} cm^2.

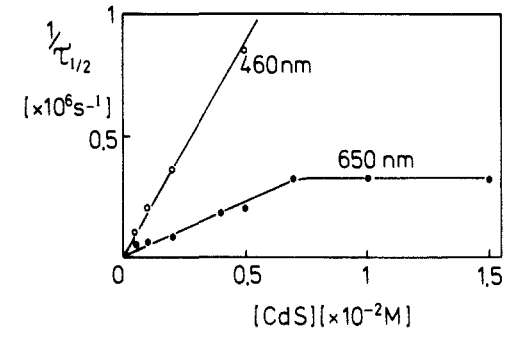

Figure 3. Reciprocal half-life of the 460-nm bleaching and the 650-nm buildup as functions of the overall CdS concentration, pH 10.

5.7 OH radicals are formed per 100 eV of absorbed radiation energy. The electrons were scavenged by N_2O also in the presence of oxygen as the solubility of N_2O is much greater than that of O_2. The N_2O–O_2 mixture was used in the experiments in which the stability of the trapped positive holes toward oxygen was to be investigated.

Results

Cadmium Sulfide. The absorption spectra of two CdS sols of different particle size are shown in the lower part of Figure 1. Note that the absorption coefficient ϵ is expressed in M_p^{-1} cm^{-1}, where M_p is the molarity of colloidal particles. Sample a consisted of larger particles with a mean diameter of 3.3 nm, as determined by electron microscopy. It begins to absorb light slightly below 515 nm, the wavelengths at which macrocrystalline CdS starts to absorb. The absorption spectrum has a weak shoulder at 460 nm. Sample b consisted of smaller particles with a mean diameter of 1.6 nm. Its absorption begins at a much shorter wavelength than that of sample a. Two absorption maxima at 300 and 280 nm and a shoulder at 250 nm can be recognized. These maxima are attributed to exciton transitions in particles of preferential agglomeration numbers.[8]

Parts a and b of Figure 2 show typical $\Delta\epsilon$ vs. time curves obtained from pulse radiolysis experiments. $\Delta\epsilon$ is defined as $(cl)^{-1} \times \log I_0/I_{(t)}$, where l is the optical length of the cell, c the concentration of OH radicals produced in the pulse, and I_0 and $I_{(t)}$ the respective light intensities before and at time t after the pulse. Depending on the wavelength, one observes an increase or a decrease in absorbance after the pulse. A final plateau of the signal was always observed at times longer than 100 μs, and this plateau persisted for the time to which measurements could be extended of several ms. $\Delta\epsilon$ in the plateau represents the difference in specific absorbancies of the products of OH attack and the starting material. At longer wavelengths, where the starting material does not absorb, $\Delta\epsilon$ is the absorption coefficient of the products. The OH radical practically does not absorb in the wavelength range investigated.

Note that wavelengths can be found (close to the beginning of light absorption) in the case of sol a at which $\Delta\epsilon$ first decreases and then increases at longer times after the pulse. This indicates

(7) Brus, L. E. *J. Chem. Phys.* **1983**, *79*, 5566–5571; **1984**, *80*, 4403–4409.
(8) Fojtik, A.; Weller, H.; Koch, U.; Henglein, A. *Ber. Bunsenges. Phys. Chem.* **1984**, *88*, 969–977.
(9) Nozik, A. J.; Williams, F.; Nenadovic, M. T.; Rajh, T.; Micic, O. I. *J. Phys. Chem.* **1985**, *89*, 397–399.
(10) Ekimov, A. I.; Onushchenko, A. A. *JETP Lett.* **1985**, *40*, 1136–9.
(11) Fischer, Ch.-H.; Weller, H.; Fojtik, A.; Lume-Pereira, C.; Janata, E.; Henglein, A. *Ber. Bunsenges. Phys. Chem.*, in press.
(12) Henglein, A.; Lilie, J. *J. Am. Chem. Soc.* **1981**, *103*, 1059–1066.
(13) Weller, H.; Fojtik, A.; Henglein, A. *Chem. Phys. Lett.* **1985**, *117*, 485–488.

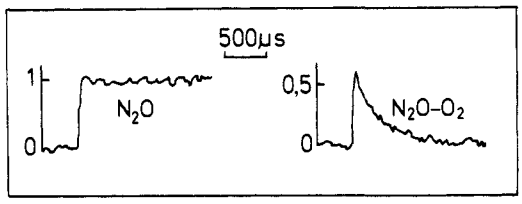

Figure 4. Time profiles of the absorbance of P_2 at 580 nm of CdS sol a (Figure 1) in the presence of N_2O and an N_2O/O_2 (80:20%) mixture.

that the reaction first leads to a product which does not absorb and which is then transformed into an absorbing species. In Figure 3, the reciprocal half-life times of the increase in absorption at a longer wavelength and of the decrease at a shorter wavelength are plotted as functions of the overall concentration of colloid a. At very low concentrations, the two half-life times are almost equal. At higher concentrations, the decay at 460 nm becomes faster much more rapidly than the buildup at 650 nm. The latter strives toward a limiting value of 3.2×10^5 s^{-1}. These effects are understood by a sequence of reactions

$$OH + CdS \xrightarrow{\tau_1} P_1 \xrightarrow{\tau_2} P_2 \qquad (2)$$

where P_1 is the first product of OH attack, which practically does not absorb, and P_2 is the absorbing second product. In the case of solution b, the life times of bleaching and buildup were always the same. The overall concentration of CdS in this solution was much lower than that in solution a, the consequence being that $\tau_2 \ll \tau_1$, i.e., the observed half-life time τ was always equal to τ_1.

The upper part of Figure 1 shows $\Delta\epsilon$ after 300 μs, i.e., after the reaction of OH + colloid was completed, as a function of the wavelength. A product P_2 is formed, which has a broad absorption band in the visible. This band is shifted toward shorter wavelengths with decreasing particle size. At wavelengths where this product has little or no absorption, $\Delta\epsilon$ is negative in the case of sol a, as some of the absorbing CdS is consumed. However, in the case of sol b, one observes oscillations in $\Delta\epsilon$. The wavelengths of the maxima of these oscillations roughly coincide with those of the minima in the spectrum of the starting material (lower part of Figure 1).

The molar conductivity of the solutions was found to be increased by 50 Ω^{-1} cm^2 with the same rate constant as the buildup of the absorbance of P_2. An increase would be expected if OH reacted via electron transfer to produce free OH^-. However, the conductivity changes were much smaller than the change of about 175 Ω^{-1} cm^2 expected for a reaction in which one OH^- is formed per OH radical.

Product P_2 was not stable in an oxygen-containing solution. Figure 4 shows a comparison of the time profiles of the 580-nm absorption for pulsed solutions containing N_2O or the N_2O–O_2 (80:20%) mixture. It is seen that the absorption decays in the presence of oxygen. The decay followed pseudo-first-order kinetics. A rate constant of 1.3×10^7 M^{-1} s^{-1} was calculated for the reaction of product P_2 with oxygen. Experiments were also made at wavelengths in the range where $\Delta\epsilon$ is negative (Figure 1). The signal was also practically constant in the presence of O_2. It is concluded that product P_2 does not significantly absorb in this wavelength range and that the negative $\Delta\epsilon$'s in Figure 1 merely result from the decrease in CdS concentration by OH attack.

Zinc Sulfide and Cadmium Phosphide. In both cases, two solutions containing particles of different size were studied. The results are presented in Figures 5 and 6. A comparison with Figure 1 shows that the observed effects are quite similar to the effects observed for CdS. A long-lived product, with an absorption band in the visible (ZnS) or the transitory range between the visible and infrared (Cd_3P_2), is produced by OH attack. As for CdS, it is observed that this absorption band is blue shifted with decreasing particle size. In the case of ZnS, reaction of the absorbing particle with oxygen was found to also occur with $k = 1.3 \times 10^7$ M^{-1} s^{-1}. In the case of Cd_3P_2, this experiment could not be carried out, since a thermal reaction of O_2 with the colloid

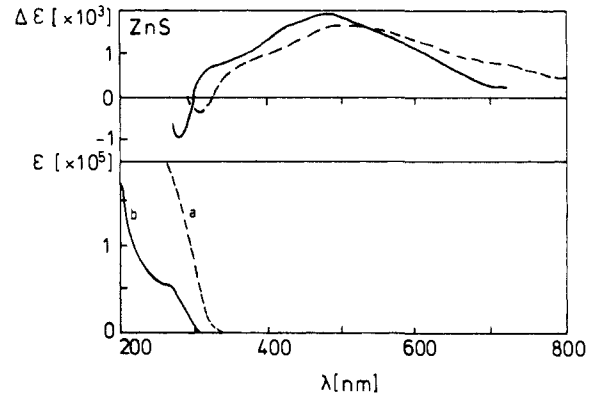

Figure 5. Absorption spectra of ZnS sols of different particle sizes (lower part) and change in specific absorbance $\Delta\epsilon$ at 50 μs after the pulse (upper part). Sol a (dashed line): 9×10^{-4} M ZnS, 1×10^{-4} M $Zn(ClO_4)_2$, 7.5×10^{-4} M $Na_6(PO_3)_6$, pH 9.0. Sol b (solid line): 1.5×10^{-4} M ZnS, 1.5×10^{-4} M $Zn(ClO_4)_2$, 2×10^{-4} M $Na_6(PO_3)_6$, pH 9.0.

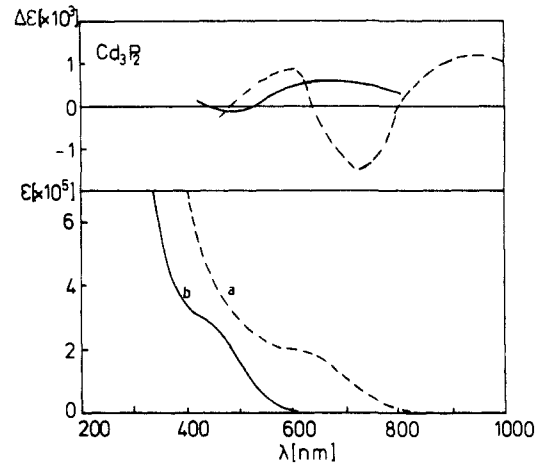

Figure 6. Absorption spectra of Cd_3P_2 sols of different particle sizes (lower part) and change in specific absorption $\Delta\epsilon$ at 500 μs after the pulse (upper part). Sol a (dashed line): 2.3×10^{-4} M Cd_3P_2, 4.1×10^{-4} M $Cd(ClO_4)_2$, 1.5×10^{-3} M $Na_6(PO_3)_6$, pH 11.6. Sol b (solid line): 8.0×10^{-5} M Cd_3P_2, 7.5×10^{-4} M $Cd(ClO_4)_2$, 1.5×10^{-3} M $Na_6(PO_3)_6$, pH 11.6.

takes place upon addition of oxygen.

Discussion

Mechanism of OH Attack. The mechanism of eq 2 explains many features of the absorption vs. time curves (Figure 2, a and b). We can attribute chemical species to the products P_1 and P_2, assuming an addition of OH to a S^{2-} anion to form P_1, followed by an electron transfer to produce S^- as product P_2, and an OH^- ion. This may be described by the equation

$$(CdS)_n + OH \xrightarrow{\tau_1} (CdS)_{n-1}CdSOH \xrightarrow{\tau_2} (CdS)_{n-1}Cd^+S + OH^- \qquad (3)$$

The S^- radical is the species which produces the broad absorption band in the visible. Similarly, in the case of Cd_3P_2, the absorbing product would be a P^{2-} radical. The S^- radical has been observed in pulse radiolysis studies of aqueous solutions of H_2S.[14] In solution it has an absorption in the ultraviolet, which is attributed to a "charge to solvent transfer" transition. In the presence of SH^-, S_2H^{2-} may be formed which has a strong absorption close to 400 nm. However, a S^- species which is part of a colloidal CdS particle may absorb light by transferring an electron into unoccupied levels of the particle and, in this way, producing an absorption band at longer wavelengths in the visible. These levels are shifted to higher energies with decreasing particle size. This

(14) Karmann, W.; Meissner, G.; Henglein, A. *Z. Naturforsch.* **1967**, *b22*, 273–282.

Table I. Calculated and Observed Half-Life τ^{650} for Various CdS Concentrations of Sol a[a]

[CdS], M	τ^{470} obsd, μs	τ^{650} obsd, μs	τ^{650} calcd, μs
5×10^{-3}	1.2	5	5
2×10^{-3}	2.7	12	7
1×10^{-3}	5	15	10
5×10^{-4}	10	18	15

[a] τ^{470} is the observed half-life of bleaching.

size quantization effect would explain why the absorption band of S^- is blue shifted with decreasing size of the colloidal particle. A similar explanation holds for the shift in the absorption of the P^{2-} species produced in the oxidation of Cd_3P_2.

The attribution of the absorption band to a trapped hole S^- would also explain its reaction with oxygen. The reaction of semioxidized sulfide anions with dissolved oxygen in illuminated CdS sols has previously been postulated.[15] It is an important step in the photoanodic corrosion of cadmium sulfide particles in aerated solution and leads to sulfate as the final product.[5,15,16] The fact that fewer OH^- ions are formed as expected from eq 2 may be explained in three ways: Either the species CdSOH does not fully dissociate, or the species Cd^+S in the colloidal particle adsorbs OH^- ions. It may finally be that a Cd^{2+} ion diffuses from the surface of a damaged colloidal particle into solution to react there with an OH^- ion to form $CdOH^+$. It is clear from these considerations that the conductometric results cannot be used as a proof for or against the mechanism of eq 2.

The limiting value of $1/\tau = 3.2 \times 10^5\ s^{-1}$ at the higher concentrations of CdS in Figure 3 (see curve for 650 nm) is interpreted as $1/\tau_2$. By using this value, reaction 2 was simulated for various CdS concentrations. Table I contains the calculated and observed values of τ_1 and τ_2 (for an observation wavelength of 650 nm). The agreement is quite satisfactory.

Oscillatory Δε. In the case of sample b in Figure 1, Δε showed some oscillatory behavior at shorter wavelengths. It may be supposed that this is somehow related to the fact that the starting material had a structured absorption spectrum. In Q-CdS of very small particle size, the wavelength at which a transition to the exciton state takes place strongly decreases with decreasing particle size.[8] As the particles become a little smaller by OH attack, their absorption maxima appear at shorter wavelengths.

Before application of a pulse of radiation, the absorbance at the optical path length of 1 cm of the solution is

$$E_0 = \epsilon_1 c_1 \tag{4}$$

ϵ_1 being the absorption coefficient of the colloidal particles (expressed in $M_p^{-1}\ cm^{-1}$, where M_p is the molarity of the particles). After the pulse, the absorbance is

$$E = \epsilon_1(c_1 - c_2) + \epsilon_2 c_2 + \epsilon_3 c_2 \tag{5}$$

where c_2 is the concentration of radicals formed. c_2 was always smaller than c_1, i.e., one colloidal particle was attacked by no more than one radical. $(c_1 - c_2)$ is the concentration of undamaged CdS particles. ϵ_2 is the absorption coefficient of the intact $(CdS)_{n-1}$ part of the damaged particles (eq 3), and ϵ_3 the absorption coefficient of the trapped hole (or S^- radical in the CdS particle, eq 3). The observed change in absorbance is

$$\Delta E = c_2(\epsilon_2 + \epsilon_3 - \epsilon_1) = c_2 \Delta\epsilon \tag{6}$$

from which Δε is calculated as

$$\Delta\epsilon = \Delta E / c_2 \tag{7}$$

At long wavelengths ϵ_1 and ϵ_2 are zero and $\Delta\epsilon = \epsilon_3$, and at wavelengths where Δε is negative or shows oscillatory behavior, $\epsilon_3 = 0$, as pointed out above. In Figure 7, the full line represents the absorption spectrum of the colloid before the pulse and the dashed line the spectrum afterwards. We assumed here that the shift due to the size quantization effect was sufficient to move the maxima into positions where the minima were located before the pulse. If Δε is measured at a wavelength λ_1, it will be slightly positive, while in a measurement at wavelength λ_2 a strong negative change in absorbance will be found. This explains in principle the oscillatory behavior of Δε.

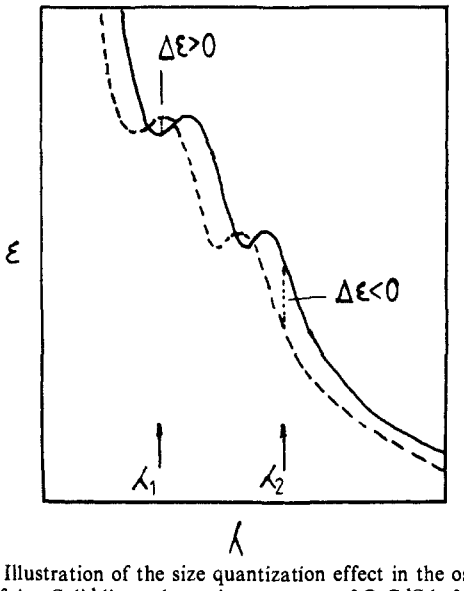

Figure 7. Illustration of the size quantization effect in the oscillatory behavior of Δε. Solid line: absorption spectrum of Q-CdS before pulse. Dashed line: assumed spectrum after pulse.

Particle Size from Pulse Radiolysis. The bimolecular rate constant of the reaction of OH with colloidal CdS is calculated from the slope of the curve at 460 nm in Figure 3 as $1.2 \times 10^8\ M^{-1}\ s^{-1}$ (M being the overall molarity of CdS). It has already been shown in the case of small silver particles[12] and more recently for small MnO_2 particles[17] that pulse radiolysis may be used to determine the size of colloidal particles. The prerequisite is a diffusion-controlled rate of the reaction of a radical with the colloid. Further, the colloidal particles are assumed to be spherical. The diameter can then be calculated from the measured second-order rate constant k:

$$d = 2\left(\frac{(3 \times 10^{-3}\ M)D}{k\rho}\right)^{1/2} \tag{8}$$

where M and ρ are the molecular weight and density of the colloidal material, respectively, and D is the diffusion coefficient of the radical. Using $k = 1.2 \times 10^8\ M^{-1}\ s^{-1}$, and for D the value of $2.0 \times 10^{-5}\ cm^2\ s^{-1}$ of water (assuming that OH has a similar rate of diffusion as H_2O),[18] one obtains $d = 3.2$ nm for sample a. k was determined as $2.0 \times 10^8\ M^{-1}\ s^{-1}$ for sample b, and from this value a diameter of the particles in this sample of 2.0 nm was calculated. These diameters agree fairly well with the mean diameters from the electron microscopic determinations. This shows that the reaction of OH with colloidal CdS is indeed diffusion controlled.

Acknowledgment. The authors acknowledge gratefully the cooperation with Dr. W. Kunath, K. Weiss, and Dr. B. Tesche, Fritz-Haber-Institut der Max-Planck-Gesellschaft, on the electron microscopic determination of particle sizes. We also thank Dr. U. Koch for assistance in these measurements.

Registry No. CdS, 1306-23-6; ZnS, 1314-98-3; Cd_3P_2, 12014-28-7; OH, 3352-57-6; H_2O, 7732-18-5; O_2, 7782-44-7; N_2O, 109-95-5.

(15) Henglein, A. *Ber. Bunsenges. Phys. Chem.* **1982**, *86*, 301–305.
(16) Meissner, D.; Memming, R.; Shuben, L.; Yesodharan, S.; Grätzel, M. *Ber. Bunsenges. Phys. Chem.* **1985**, *89*, 121–124.
(17) Lume-Pereira, C.; Baral, S.; Henglein, A.; Janata, E. *J. Phys. Chem.*, in press.
(18) "Landolt-Börnstein, Zahlenwerte und Funktionen"; Springer-Verlag: Berlin, Heidelberg, New York, 1969; Band II, Teil 5, p 581.